Excited state properties of liquid water

2009 J. Phys.: Condens. Matter 21 033101

(http://iopscience.iop.org/0953-8984/21/3/033101)

J. Phys.: Condens. Matter **21** (2009) 033101 (15pp) doi:10.1088/0953-8984/21/3/033101

TOPICAL REVIEW

Excited state properties of liquid water

Viviana Garbuio[1], **Michele Cascella**[2] **and Olivia Pulci**[1]

[1] European Theoretical Spectroscopy Facility (ETSF), CNR-INFM-SMC, Department of Physics University of Rome Tor Vergata, Italy
[2] Departement für Chemie und Biochemie, Laboratory of Computational Chemistry and Biochemistry, Universität Bern, Switzerland

Received 11 July 2008, in final form 17 October 2008
Published 11 December 2008
Online at stacks.iop.org/JPhysCM/21/033101

Abstract
In this paper, we give an overview of the state of the art in calculations of the electronic band structure and absorption spectra of water. After an introduction to the main theoretical and computational schemes used, we present results for the electronic and optical excitations of water. We focus mainly on liquid water, but spectroscopic properties of ice and vapor phase are also described. The applicability and the accuracy of first-principles methods are discussed, and results are critically presented.

(Some figures in this article are in colour only in the electronic version)

Contents

1. Introduction

Water is the most common liquid substance on the Earth's surface. Its crucial involvement in many fundamental processes, in particular, the development of life, makes liquid water one of the most intriguing and extensively studied systems from both a theoretical and experimental point of view. Although the isolated *in vacuo* molecule of water is a very simple system, many basic aspects of this substance, even its structure in the liquid phase, are still subject to debate [1–15]. In the last twenty years of the last century, different theoretical studies investigated the structure and dynamics of liquid water and ions derived from its auto-protolysis or from photo-dissociation, building up reliable models able to shed light on quantities like neutron diffraction, diffusion coefficients and viscosity [16–26]. Lots of theoretical works have also focused on the roto-vibrational excitations and on the stretching of the OH bond for small water clusters [27–38], in liquid water [21], for the water–hydroxyl complex [39–43] and for the hydronium–water complex [20, 44].

The electronic properties of water as a solvent are extremely interesting since water can influence many electronic events (electron transfer, photo-excitation) of solute molecules by its dielectric response [45, 46] or by actively participating in electronic processes, i.e. in electron-transfer phenomena at biological interfaces [47].

Despite some pioneering studies [22, 48–50], the high computational cost needed to address the modeling of a disordered system such as a liquid substance limited, in those years, the studies of the electronic structures and properties to the gaseous phase [51, 52] or to crystalline ice [53, 54].

In the present decade, aided by the rapid increase in computational power, a series of theoretical works on the

electronic properties of liquid water have appeared and will be discussed in the following sections.

The main difficulty in producing reliable theoretical predictions of the electronic properties of water lies in the necessary compromise between the level of accuracy at which the system can be described and the thorough sampling of the phase-space, as required for converged computational quantities.

Authors of published works on the subject have profited from three possible methodologies. The first choice lies in sampling structures at a lower level (e.g. molecular mechanics), and then performing high level single-point electronic structure calculations on them. The second possibility is to use hybrid Hamiltonians (usually referred to as QM/MM schemes), where only a portion of the system, typically a single water molecule, is described at the quantum level, while the rest is treated at a molecular mechanics level. The third kind of calculation present in the literature concerns first-principles molecular dynamics, where the full system, including its electronic degrees of freedom, undergoes time-evolution.

In the present paper, after a brief introduction to the various methods, we shall give an overview of the state of the art in the subject, highlighting some of the major results that have been achieved by the community in ground state response properties (polarizability tensors, dielectric constants), and excited state calculations. However, this work does not intend to represent an exhaustive review of the subject, as an enormous range of material and open questions remain.

2. Methods

Liquid water is characterized by strong dipolar interactions and by a network of hydrogen bonds; hence, a correct description of its electronic structure requires methods able to accurately account for long-range polarization and short-range correlation effects.

The general problem of n electrons interacting in the presence of N nuclei, within the Born–Oppenheimer approximation [55], takes the form:

$$H\Psi(\{\mathbf{r}\}) = E\Psi(\{\mathbf{r}\}) \tag{1}$$

where $\Psi(\{\mathbf{r}\})$ is the electronic wavefunction and H is the electronic Hamiltonian (in atomic units):

$$\begin{aligned} H &= -\frac{1}{2}\sum_i \nabla^2_{\mathbf{r}_i} - \sum_{i,I}\frac{Z_I}{|\mathbf{r}_i - \mathbf{R}_I|} + \frac{1}{2}\sum_{i\neq j}\frac{1}{|r_i - r_j|} \\ &= T + V_{\text{ext}} + V_{\text{e-e}}. \end{aligned} \tag{2}$$

Evaluation of the exact eigenvalues and eigenstates of such a Hamiltonian is too expensive a task for polyatomic molecular systems, and therefore it is required to introduce further approximations in order to obtain some knowledge about these many-body problems.

Various methods address the problem through different approaches: by reducing the problem to the study of single-particle Hamiltonians, as in Hartree [56] and Hartree–Fock [57] methods, or by exploiting the variational principle with more complicated wavefunction sets, or by focusing attention on the electronic density instead of the many-body wavefunction, as in density functional theory and time-dependent density functional theory.

An additional problem regarding the calculations of (excited state) properties of water lies in its liquid nature. Several strategies have been considered to simplify the study of disordered systems: use of clusters of increasing size to model the liquid, 'mean-field' approaches (implicit solvent, e.g. dielectric continuum), use of periodically repeated small unit cells, and hybrid QM/MM approaches, which use different combinations of quantum and classical methods to describe the two subsystems.

2.1. Wavefunction based methods

Several methods try to solve the electronic problem presented by equation (1) by choosing suitable approximate wavefunctions. The simplest *ansatz* for $\Psi(\{\mathbf{r}\})$ is the Hartree–Fock (HF) determinant,

$$\Psi \approx \Phi_0 = \text{Det}[\varphi(1)\varphi(2)\cdots\varphi(n)], \tag{3}$$

where the single-particle orbitals $\varphi(i)$ are optimized altogether through an iterative self-consistent procedure. This mean-field solution does not take into account electronic correlation and it is usually used just as a starting point for more accurate calculations. Therefore, published works that have made use of wavefunction based methods are typically based on Møller–Plessett perturbation series (MP2, MP4), on configuration interaction (CI), or on coupled-cluster (CC) theory. The general theory behind such methods is widely described in text-books of quantum chemistry (see for example [58]), and therefore is just briefly recalled here.

2.1.1. Configuration interaction. The most straightforward method for improving the HF solution is to build a series of Slater determinants where not only the n lowest energy (occupied) φ are used, but *virtual* (unoccupied) orbitals are also included. In this way, the solution to equation (1) reads:

$$\Psi = t_0\Phi_0 + \sum_i^{\text{occ}}\sum_a^{\text{vir}} t_i^a\Phi_i^a + \sum_{i<j}^{\text{occ}}\sum_{a<b}^{\text{vir}} t_{ij}^{ab}\Phi_{ij}^{ab} + \cdots \tag{4}$$

where Φ_i^a represents all possible *singly excited* determinants, that is, a Slater determinant obtained by substituting one φ in the HF determinant by a virtual one; Φ_{ij}^{ab} represents all possible *doubly excited* determinants; and so on. The various t_i coefficients are then optimized according to the variational principle. This method is known as configuration interaction [59] (CI). The expansion in equation (4) (known as the *full-CI* solution) is not affordable from a computational point of view, and therefore truncated CI methods have to be applied. The most drastic simplification implies taking only single excitations (CIS) into account. In fact, for the variational properties of the HF determinant, the matrix element $\langle\Phi_0|H|\Phi_i^a\rangle$ is zero, and therefore, such a truncation cannot improve the ground state, while it may be used for

approximate excited state calculations. Methods including further excitations take their name accordingly (CISD: CI with single and double excitations; CISDT: CI with single, double and triple excitations, etc).

2.1.2. Multiconfiguration methods. In multiconfigurational self-consistent field (MCSCF) [60] approaches, not only are the coefficients in the expansion of equation (4) optimized, but also the single-particle orbitals. The major drawback of such a technique is that stationary points of the variational procedure are problematic, since convergence to local maxima or saddle points are more likely to occur than in other SCF procedures. Despite these convergence problems, such a treatment allows calculation of *static correlation* in the system. The major problem of MCSCF methods is in the initial choice of the different electronic configurations that have to be included for a correct study of the properties of interest. One of the most used approaches is the complete active space self-consistent field (CASSCF) [61]. Within this scheme, the single-particle orbitals are partitioned into *active* and *inactive* spaces. Active space orbitals (that have to be arbitrarily chosen; typically, some of the highest occupied and the lowest unoccupied orbitals) undergo a full-CI cycle, and are then included in an MCSCF optimization. The most complex multiconfigurational method is the so-called multi-reference configuration interaction (MRCI), which consists of writing a CI expansion starting from a MCSCF wavefunction, rather than a single HF determinant.

2.1.3. Coupled cluster. Let us define an excitation operator T as:

$$T = T_1 + T_2 + \cdots + T_n + \ldots. \tag{5}$$

This operator is such that any T_i acts on an HF-reference determinant Φ_0, to generate all possible ith excited determinants:

$$\begin{aligned} T_1\Phi_0 &= \sum_{i}^{\text{occ}}\sum_{a}^{\text{vir}} t_i^a \Phi_i^a \\ T_2\Phi_0 &= \sum_{i<j}^{\text{occ}}\sum_{a<b}^{\text{vir}} \Phi_{ij}^{ab} t_{ij}^{ab} \end{aligned} \tag{6}$$

where Φ_i^a defines a singly excited Hartree–Fock determinant, Φ_{ij}^{ab} a doubly excited one and so on.

From this definition, the CI wavefunction can be rewritten as:

$$\Phi_{\text{CI}} = (1 + T)\Phi_0. \tag{7}$$

In coupled-cluster theory (CC), the optimized CC wavefunction is instead derived starting from the definition of the operator e^T:

$$e^T = 1 + T + \frac{1}{2}T^2 + \frac{1}{6}T^3 \cdots = \sum_i \frac{1}{i!}T^i. \tag{8}$$

The operator e^T can be applied to Φ_0 to produce the CC wavefunction Φ_{CC}:

$$\begin{aligned} \Phi_{\text{CC}} = e^T\Phi_0 = \Big[1 + T_1 + \left(T_2 + \tfrac{1}{2}T_1^2\right) \\ + \left(T_3 + T_2T_1 + \frac{1}{3!}T_1^3\right) + \cdots\Big]\Phi_0. \end{aligned} \tag{9}$$

The Schrödinger equation for the CC wavefunction reads:

$$He^T\Phi_0 = E_{\text{CC}}e^T\Phi_0. \tag{10}$$

Solution of equation (10) can be obtained by projecting the reference HF determinant on both sides of the equation. This operation leads to:

$$\begin{aligned} \langle\Phi_0|H|\Phi_{\text{CC}}\rangle &= E_{\text{CC}}\langle\Phi_0|\Phi_{\text{CC}}\rangle \\ \left\langle\Phi_0|He^T|\Phi_0\right\rangle &= E_{\text{CC}}\langle\Phi_0|1 + T_1 + \cdots|\Phi_0\rangle \\ E_{\text{CC}} &= \left\langle\Phi_0|He^T|\Phi_0\right\rangle. \end{aligned} \tag{11}$$

From the orthogonality properties of the HF orbitals, and from the fact that the Hamiltonian operator contains only one- or two-body interactions, equation (11) simplifies into:

$$\begin{aligned} E_{\text{CC}} = E_0 + \sum_{i}^{\text{occ}}\sum_{a}^{\text{vir}} t_i^a \left\langle\Phi_0|H|\Phi_i^a\right\rangle \\ + \sum_{ij}^{\text{occ}}\sum_{ab}^{\text{vir}} \left(t_{ij}^{ab} + t_i^a t_j^b - t_i^b t_j^a\right)\left\langle\Phi_0|H|\Phi_{ij}^{ab}\right\rangle \end{aligned} \tag{12}$$

where E_0 is the Hartree–Fock energy, indices (i, j) run over occupied orbitals and indices (a, b) over virtual ones. The first sum in equation (12) contains single-excitation determinants, and therefore is zero for the Brillouin theorem, while the second elements correspond to two-electron Coulomb integrals over HF molecular orbitals. Therefore, equation (12) can be reduced to:

$$\begin{aligned} E_{\text{CC}} = E_0 + \sum_{i<j}^{\text{occ}}\sum_{a<b}^{\text{vir}}(t_{ij}^{ab} + t_i^a t_j^b - t_i^b t_j^a) \\ \times \left(\langle\varphi_i\varphi_j|\frac{1}{r_{12}}|\varphi_a\varphi_b\rangle - \langle\varphi_i\varphi_j|\frac{1}{r_{12}}|\varphi_b\varphi_a\rangle\right) \end{aligned} \tag{13}$$

where φ are single electron molecular orbitals. It results in the CC energy being the HF energy plus a correlation contribution, which arises entirely from the coefficients of single and double excitations and from two-electron integrals.

The coefficients of the CC expansion are derived with a procedure similar to the one applied for the energy. In fact, by multiplying equation (10) by a singly excited determinant Φ_k^l, and expanding the exponential operator, one gets:

$$\begin{aligned} \left\langle\Phi_k^l\left|He^T\right|\Phi_0\right\rangle &= E_{\text{cc}}\left\langle\Phi_k^l\left|e^T\right|\Phi_0\right\rangle \\ \left\langle\Phi_k^l\left|H(1 + T_1 + T_2 + \cdots)\right|\Phi_0\right\rangle &= \left\langle\Phi_k^l\left|T_1\right|\Phi_0\right\rangle \end{aligned} \tag{14}$$

$$\begin{aligned} \left\langle\Phi_k^l\left|HT_1\right|\Phi_0\right\rangle + \left\langle\Phi_k^l\left|HT_2\right|\Phi_0\right\rangle + \tfrac{1}{2}\left\langle\Phi_k^l\left|HT_1^2\right|\Phi_0\right\rangle \\ + \left\langle\Phi_k^l\left|HT_3\right|\Phi_0\right\rangle + \left\langle\Phi_k^l\left|HT_1T_2\right|\Phi_0\right\rangle \\ + \tfrac{1}{6}\left\langle\Phi_k^l\left|HeT_1^3\right|\Phi_0\right\rangle = E_{\text{cc}}\left\langle\Phi_k^l\left|T_1\right|\Phi_0\right\rangle. \end{aligned} \tag{15}$$

Due to orthogonality of Slater determinants, all other contributing integrals that should appear in the expansion are zero. These terms form a set of coupled equations which link single-excitation coefficients to single, double, and triple ones. Therefore, although triple-excitation coefficients do not appear in the expression for the CC energy (see equation (13)), they are required to solve equations for the single excitations. Similar procedures have to be applied to generate higher-order coefficients.

These expressions, although formally exact, have to be truncated for obvious computational reasons. This is done by reducing the operator T to a limited number of excitations. Defining $T \approx T_1$ does not lead to any improvement of the HF energy, as matrix elements between HF and singly excited orbitals are zero. Therefore, the first approximation for CC typically used is $T \approx T_1 + T_2$. Such truncation, known as CCSD (coupled-cluster singles and doubles), already scales as N^8, and therefore signs the limit for average-size molecules. Possible methods to improve CC results, broadly used nowadays, are to include higher-order excitation in a perturbative scheme. Such methods are typically indicated as CCSD(T) or CCSD(TQ) (according to which excitations are introduced by perturbation theory) [62].

2.2. Density functional based methods

Density functional theory (DFT) and time-dependent density functional theory (TDDFT) aim at solving the many-body problem in terms of the one-particle electronic density alone instead of the more complex many-body wavefunction $\Psi(r_1, \ldots, r_N)$. The seminal paper of Hohenberg and Kohn [63] in 1964 and the subsequent work of Kohn and Sham (KS) [64] in 1965 lay the foundations for DFT. For a detailed review on DFT see, for example, [65]. The generalization of DFT to arbitrary time-dependent systems was given by Runge and Gross [66] in 1984, and opened the way towards time-dependent DFT calculations; reviews of this theory can be found in [67–69].

2.2.1. Density functional theory. DFT is based on the Hohenberg–Kohn theorem which asserts that all the ground state properties of an interacting electronic system, including the total energy E, can be expressed as unique functionals of the electronic density alone:

$$E[n(\mathbf{r})] = F[n] + \int \mathrm{d}\mathbf{r}\, V_{\mathrm{ext}}(\mathbf{r}) n(\mathbf{r}) \geqslant E_{\mathrm{GS}} \qquad (16)$$

where E_{GS} is the ground state energy of the system, and $F[n] = T + V_{\mathrm{ee}}$ is a universal functional that contains the contribution of the kinetic (T) and electron–electron (V_{ee}) part of the Hamiltonian. A scheme for resolving this problem was presented by Kohn and Sham [64], who introduced a fictitious non-interacting system of particles having the same electronic density as the real system. Within this single-particle scheme, they obtained a set of self-consistent single-particle equations:

$$[-\tfrac{1}{2}\nabla^2 + V_{\mathrm{ext}} + V_{\mathrm{H}} + V_{\mathrm{xc}}]\phi_i(\mathbf{r}) = \varepsilon_i \phi_i(\mathbf{r}) \qquad (17)$$

where V_{xc} is the exchange and correlation potential, V_{H} is the Hartree potential and

$$n(r) = \sum_i f_i |\phi_i(\mathbf{r})|^2 \qquad (18)$$

with f_i being the occupation number of the state i. Although in principle exact, the functional form of the exchange and correlation potential is unknown and, therefore, it has to be approximated.

Different kinds of approximations for the exchange and correlation (xc) functional, based on density alone (local density approximation (LDA)) [64], density gradients (generalized gradient approximation (GGA)) [70–75], hybrid exact-exchange [76], or kinetic energy [77] are typically used.

Special care has to be taken in the choice of the xc-functional when dealing with the energetic of hydrogen-bonded systems [78, 79]. Moreover, nowadays DFT exchange and correlation functionals fail in accurately describing van der Waals interactions. New important developments have appeared in the literature (see, for example, [80–86]), leading to promising results.

2.2.2. Time-dependent density functional theory (TDDFT). Considering a time-dependent Hamiltonian $H(t) = T + V_{\mathrm{ext}}(t) + V_{\mathrm{e-e}}$, the system will be described by a time-dependent Schrödinger equation

$$H(t)\Psi(t) = \mathrm{i}\frac{\partial}{\partial t}\Psi(t), \quad \text{with initial state} \quad \Psi(t_0) = \Psi_0. \qquad (19)$$

In analogy with the Hohenberg–Kohn–Sham theory, it can be shown that an invertible map between the time-dependent external potential and the electronic density $n(\mathbf{r}, t)$ exists up to an additive purely time-dependent function, $c(t)$, in the potential. At the same time, the time-dependent wavefunctions are unique functionals of the density, up to a purely time-dependent phase which cancels out when taking the expectation value of an operator. Moreover, instead of searching for the exact ground state density through the variational minimization of the total energy (as in DFT), in TDDFT the time-dependent Schrödinger equation (19) corresponds to a stationary point of the action integral A (functional of the density):

$$A[n] = \int_{t_0}^{t_1} \mathrm{d}t \langle \Psi(t) | \mathrm{i}\frac{\partial}{\partial t} - H(t) | \Psi(t) \rangle. \qquad (20)$$

The last analogy between stationary and time-dependent DFT concerns the introduction of an auxiliary non-interacting particle system having the same density as the interacting one; this leads to the following equation:

$$\left[\mathrm{i}\frac{\partial}{\partial t} + \frac{1}{2}\nabla^2\right]\phi(\mathbf{r}, t) = V_{\mathrm{eff}}(\mathbf{r}, t)\phi_i(\mathbf{r}, t) \quad \text{with}$$
$$n(\mathbf{r}, t) = \sum_i^{\mathrm{occ}} \phi_i^*(\mathbf{r}, t)\phi_i(\mathbf{r}, t), \qquad (21)$$

where the effective potential contains an exchange and correlation contribution $V_{\mathrm{xc}}(\mathbf{r}, t)$.

In time-dependent linear response theory, the response function χ (which measures the degree to which the density responds to first order in the external potential) satisfies the Dyson-like equation:

$$\chi(\mathbf{r}, \mathbf{r}', \omega) = \chi_0(\mathbf{r}, \mathbf{r}', \omega) + \int \mathrm{d}\mathbf{r}_1\, \mathrm{d}\mathbf{r}_2 \chi_0(\mathbf{r}, \mathbf{r}_1, \omega) K(\mathbf{r}_1, \mathbf{r}_2, \omega) \chi(\mathbf{r}_2, \mathbf{r}', \omega) \qquad (22)$$

with $K(\mathbf{r}_1, \mathbf{r}_2, \omega) = V(\mathbf{r}_1, \mathbf{r}_2) + f_{\rm xc}(\mathbf{r}_1, \mathbf{r}_2, \omega)$ where V is the Coulomb potential and $f_{\rm xc}$ is the exchange and correlation kernel, defined as

$$f_{\rm xc}(\mathbf{r}, \mathbf{r}', t, t') = \frac{\delta V_{\rm xc}(\mathbf{r}, t)}{\delta n(\mathbf{r}', t')}. \tag{23}$$

The exchange–correlation potential is unknown, hence $f_{\rm xc}$ has to be approximated in some way. Incidentally, putting $f_{\rm xc} = 0$ in equation (22) corresponds to performing a random phase approximation (RPA) calculation. A common approximation for $f_{\rm xc}$ is the adiabatic local density approximation (ALDA, often called TDLDA) which considers $f_{\rm xc}$ as the functional derivative of the static LDA exchange and correlation potential. It has turned out that TDLDA often yields good optical spectra for finite systems (see for example [87]) but fails to describe solids (where no improvement with respect to a standard RPA calculation is found, see for example [88–91]), surfaces [92], molecular chains [93], liquid water [94], molecular solids [95] and, in general, extended systems. This is due to the wrong asymptotic behavior of the ALDA kernel [96]. Several attempts to go beyond a local scheme have been proposed in recent years and a great deal of effort has been devoted towards finding efficient and reliable non-local (in space and in time) approximations (for a review, see for example [97]).

2.3. Green's function based methods

Green's function theory is particularly suitable for studying excited state properties and hence for interpreting or predicting spectroscopic experimental results. Details of the theory can be found, for example, in [69, 98].

2.3.1. Quasi-particle equations. In the Lehmann representation, it can be shown that the poles of the Green's function are the electron addition and removal energies, that is, the energy levels of unoccupied and occupied states, respectively, as measured for example in inverse and direct photoemission experiments. For practical calculations, a single-particle-like framework is regained by introducing the concept of quasi-particles (QP) which can be thought of as real particles plus a polarization cloud, due to electron–hole pairs, surrounding them and screening the mutual interaction. The difference between 'bare' particles (subject only to the Hartree potential) and quasi-particles can be accounted for by the self-energy operator Σ which is a non-local, non-Hermitian, energy-dependent operator.

A Schrödinger-like equation for the QP can be written:

$$H_0(\mathbf{r})\psi_n(\mathbf{r}, \omega) + \int d\mathbf{r}' \Sigma(\mathbf{r}, \mathbf{r}', \omega)\psi_n(\mathbf{r}', \omega) = E_n(\omega)\psi_n(\mathbf{r}, \omega), \tag{24}$$

where $H_0(\mathbf{r}) = -\frac{1}{2}\nabla^2_{\mathbf{r}} + V_{\rm ext}(\mathbf{r}) + V_H(\mathbf{r})$; an adequate expression for Σ has to be found.

2.3.2. GW approximation. It can be shown that the QP equation is equivalent to a Dyson-like equation for the Green's function:

$$G(1,2) = G_0(1,2) + \int d(34)\ G_0(1,3)\Sigma(3,4)G(4,2).$$

This is the first equation of a closed set of five equations proposed by Hedin [99, 100], the others being:

$$\Sigma(1,2) = i\int d(34)\ G(1,3)\Gamma(3,2,4)W(4,1^+);$$

$$W(1,2) = V(1,2) + \int d(34)\ W(1,3)P(3,4)V(4,2);$$

$$P(1,2) = -i\int d(34)\ G(1,3)G(4,1^+)\Gamma(3,4,2);$$

$$\Gamma(1,2,3) = \delta(1,2)\delta(1,3) + \int d(4567)\ \frac{\delta\Sigma(1,2)}{\delta G(4,5)}G(4,6)G(7,5)\Gamma(6,7,3);$$

where 1^+ stands for $(\mathbf{r}_1, \sigma_1, t_1 + \delta)$ and δ is an infinitesimal positive number. This set of equations also involves the time ordered polarization operator $P(1,2)$, the dynamical screened Coulomb interaction $W(1,2)$ and the vertex function $\Gamma(1,2,3)$. These equations must be solved self-consistently to obtain the exact solution, a procedure that is practically impossible for realistic systems and hence some simplifications have to be found. The simplest approximation consists of starting with a non-interacting system with $\Sigma = 0$; in this case $G = G_0$, the vertex correction is neglected and $P(1,2) = -iG_0(1,2)G_0(2,1)$. Hence the self-energy becomes

$$\Sigma(1,2) = iG_0(1,2)W_0(2,1^+). \tag{25}$$

This is the so-called GW approximation. In principle more iterations should be performed but calculations usually stop at this first step (one-shot GW), and obtain quite accurate results for one-particle excitations. Furthermore, the underestimation of the band gap, a peculiarity of DFT, is usually removed.

2.3.3. Bethe–Salpeter equation. With regards to absorption spectra, it is important to take into account the interactions between holes and electrons by means of the inclusion of vertex corrections. This can be achieved through a second iteration of Hedin's equations, which gives for the vertex the expression

$$\Gamma(123) = \delta(12)\delta(13) + iW(1^+2)\int d(67)G(16)G(72)\Gamma(673). \tag{26}$$

This equation can be transformed into an integral equation for a four-point generalized polarizability by introducing four-point quantities, i.e. ${}^4P(1234)$, ${}^4W(1234) = W(12)\delta(13)\delta(24)$ and ${}^4P_0(1234) = P_0(12)\delta(13)\delta(24)$. The Bethe–Salpeter equation for the polarizability can then be derived and gives:

$${}^4P = {}^4P_0 + {}^4P_0K{}^4P. \tag{27}$$

The kernel K is made of two terms: an electron–hole exchange contribution involving the bare potential V, and the electron–hole attraction due to the screened potential W, i.e.

$$K(1234) = \delta(12)\delta(34)V(13) - \delta(13)\delta(24)W(12). \tag{28}$$

In practical calculations, an effective two-particle excitonic Hamiltonian is constructed. The eigenfunctions and eigenvalues of this Hamiltonian build up the absorption

spectrum. The neutral excited states of the system are now represented as a linear combination of electron–hole couples and the position and shape of the absorption spectrum are deeply modified with respect to the independent quasi-particle spectrum. Details of its derivation can be found in [69].

It is very interesting to notice that the Bethe–Salpeter and the TDDFT equation can be put on the same footing, since both can be schematically written in a Dyson-like form:

$$S = S_0 + S_0 K S. \tag{29}$$

The similarity is only formal, since S is a two-point polarizability $\chi(12)$ in the TDDFT case, or a four-point generalized polarizability $P(1234)$ in the case of the BSE. Moreover, S_0 is the Kohn–Sham independent particle response function χ_0 in the TDDFT scheme, whereas in the many-body approach it represents the independent quasi-particle response function (calculated using quasi-particle, hence GW, eigenvalues). Finally, the kernels K are obviously different since one contains the f_{xc} TDDFT kernel whereas, in the BSE case, the screened interaction W appears. This formal similarity is important, and it has been at the basis of several theoretical developments in the search of a TDDFT kernel based on the many-body perturbation approach [88–90].

2.4. Hybrid methods (QM/MM)

Wavefunction based methods for the solution of the many-electron problem typically make use of localized basis sets (e.g. Gaussians). Therefore, they are intrinsically suited to the study of finite-size molecular systems, rather than to the study of extended moieties, such as compounds in any condensed phase, and hence necessary approximations have to be introduced. After the first pioneering works in the field [101, 102], in the last years hybrid quantum mechanics/molecular mechanics (QM/MM) models have been successfully implemented and used to study a variety of molecular systems in the condensed phase, from molecules in solution to active sites in proteins to surfaces.

QM/MM models are based on an *ad hoc* partitioning of the system of interest into two regions, each studied at a different level of theory. The QM region is treated at the quantum level of theory, while the MM region, typically much larger than the QM one, is described by a simpler parameterized Hamiltonian.

Formally, the QM/MM Hamiltonian is written as:

$$H = H_{QM} + H_{MM} + H_{QM/MM} \tag{30}$$

where H_{QM} and H_{MM} are the Hamiltonians of the QM and MM regions, respectively, and $H_{QM/MM}$ is the term needed to consider the interactions between the QM and the MM parts. The $H_{QM/MM}$ term can take different forms according to the coupling method adopted (e.g. subtractive *molecular embedding* [103, 104], or additive *full-Hamiltonian* schemes [105]), and to the various QM approaches used to describe the QM region.

QM/MM protocols present in the papers discussed in this review comprise: (i) additive methods for coupled-cluster (CC) [106], and multiconfigurational self-consistent-field calculations [107], (ii) polarizable force-fields, discrete reaction field and frozen-density embedding schemes coupled to time-dependent density-functional-theory (TDDFT) [108], or (iii) perturbative methods applied to different QM calculations (TDDFT, CC, (CASSCF)) [109].

3. The structure of liquid water

Calculations of excited state properties of liquid water obviously require, as initial input, the structure of the liquid itself. A vast series of experimental data on water, probing structural, thermodynamic and dynamical properties, points at a tetrahedral hydrogen-bonding network as the reliable structure of liquid water [110]. This structure has been broadly confirmed both by classical molecular dynamics [111–114] and by first-principles [21, 22, 115] simulations. However, recent x-ray absorption spectroscopy (XAS) experiments have challenged such structure. In fact, based on these experiments, Wernet *et al* [1] proposed a model for liquid water where each water molecule has only two H-bonded first neighbors, resulting in a hydrogen-bonding network that replaces the tetrahedral structure with chains of water molecules instead [1, 8]. Such structures, to date, have not been reproduced by any dynamical model of liquid water, and have been questioned by a series of works (see, e.g. [6, 9–11]). The debate about these experiments in particular [12–15], and more broadly, about the structure of water, is ongoing and still a very hot topic in the community. Although a very fascinating subject, it is outside the subject of the present review, devoted to the excited state properties of water, and therefore we shall not discuss it further.

4. Molecular properties

In the presence of an electrostatic field, the energy of a molecule can be expanded in terms that contain the multipolar moments, dipole polarizability, and the first-and higher-order hyperpolarizabilities. Most of these terms have not been determined experimentally for liquid water. Therefore, reliable computational predictions for these terms are needed in order to study general phenomena involving linear response to any kind of electric/electronic perturbation. Here we review the most recent studies on both static ground state and electrical response properties of water.

4.1. Multipole moments

The dipole moment of water was inferred from a series of experimental studies both for the isolated molecule and in solution. In particular, the dipole of the isolated water molecule was determined from Stark effect measurements [116] and more recently by molecular beam electric resonance spectroscopy [117] yielding a value of 1.855 D, while the dipole in the full liquid environment increases to ≈2.4–2.6 D [118]. Such a change in the dipole intensity, moving from the gas to the condensed phase, must be related to the polarization of the water molecules, and has been the object of different theoretical studies in the last twenty years. Predicted values of the dipole moment are quite robust and independent

of the level of theory used. In particular, full *ab initio* [22] and QM/MM [119] molecular dynamics simulations based on GGA/DFT reported a value of 2.7 D, the exact value being strongly dependent on the instantaneous configuration of the water molecules. A more recent joint experimental–theoretical work [120] (MP2/aug-cc-VDZ level of description) on water clusters showed that the water dipole already reaches the typical value of the condensed phase for the $(H_2O)_6$ species. Batista *et al* [121] worked on water clusters and ice Ih, and pointed out the importance of choosing correct schemes for charge density partitioning to get reliable results.

Gubskaya and Kusalik [122] determined dipole and quadrupole moments using a mean-field approach, where the effect of the solvent surrounding one single quantum water molecule (treated at MP2/MP4 level of theory) is modeled by a local electric field. The nature of this local field is determined by average distributions obtained from MD simulations. The dipole moment reported in their work is in agreement with the experiment. They report the diagonal elements of the quadrupole moment, finding some discrepancies depending on the level of theory (MP2 or MP4), and on the different mean-fields applied to the quantum water.

In more recent years, theoretical investigations made use of hybrid QM/MM methods to determine both the dipole moment and the higher-order quadrupole tensor. A series of works by Mikkelsen and co-workers [107, 123] have accurately studied the effect of the environment around the QM portion, showing that more accurate results require the inclusion of explicit polarization terms in the Hamiltonian describing the MM part. Specifically, they found that a non-polarizable description of the MM portion leads to an underestimation of the dipole moment of about 9%, while the shift in the dipole moment from gas to liquid phase is underestimated by about 29%. Inclusion of explicit polarization terms in the MM Hamiltonian leads to values closer to experiment and former theoretical predictions. They reported values of 2.74 D for a CCSD(aug-cc-pVQZ) description in the QM part and 2.71 D for MCSCF(aug-cc-pVQZ).

Jensen and co-workers have used a discrete solvent reaction field model combined with DFT [108, 124]. Their results are in agreement with those of Mikkelsen, showing that the total dipole moment of liquid water in hybrid models is well reproduced only if a polarization term is included in the MM part. Interestingly, Jensen *et al* showed that the dipole moment of water can be reproduced in good agreement with CCSD results using a LDA xc-functional [108]. The same groups reported values for the diagonal elements [123, 124] and the full quadrupole tensor [125]. In all these calculations, the water molecule in the QM part is placed in the xz plane with the oxygen at the origin and the z axis bisecting the HOH angle. Unlike the dipole, the quadrupole of liquid water has not been determined experimentally. However, these sets of calculations report similar values for the diagonal quadrupole elements: $\mathbf{Q}_{xx} = 2.08$ au [124], 2.09 au [125], $\mathbf{Q}_{yy} = -2.17$ au [124], -2.16 au [125], and $\mathbf{Q}_{zz} = 0.08$ au [124, 125].

4.2. Polarizability

The static mean dipole polarizability ($\bar{\alpha}$) of water *in vacuo* is known from dipole oscillator strength distribution experiments [126]. First (β) and second (γ) hyperpolarizabilities can be derived from Kerr effect measurements and the electric field induced second harmonic generation technique (ESHG), and were reported by Ward and Miller [127] and more recently by Kaatz *et al* [128].

No experimental data are available for $\bar{\alpha}$ of liquid water, while $\bar{\beta}$ and $\bar{\gamma}$ were derived by Levine and Bethea via ESHG experiments [129]. Water polarizabilities in gaseous clusters were studied in the late 1990s by Otto *et al* [130] by means of coupled Hartree–Fock calculations, and by Rodriguez *et al* [131] via DFT calculations. An extensive study of the full (static) α, β, γ tensors of the water dimer has been proposed by Maroulis [132]. In his work, he studied the convergence of the values of these tensors from different methodologies (from HF, to MP2/MP4, to CCSD(T)), different basis sets, and relaxation of the molecular structure. He found that hyperpolarizability tensors are strongly dependent on electron-correlation effects, while the water geometry does not influence the results so much. He also found that Møller–Plessett expansions perform reasonably well, as compared to more expensive CCSD(T) calculations.

Gubskaya and Kusalik's mean-field approach [122] to simulate the condensed phase condition reports only a small variation of the value of $\bar{\alpha}$ with respect to the *in vacuo* situation, while they observe a dramatic increase for $\bar{\beta}$ and $\bar{\gamma}$—reporting also a change in sign for $\bar{\beta}$—in agreement with experiment.

The two parallel series of works by Mikkelsen, Christiansen, and co-workers [107, 125, 133–138] and Jensen and co-workers [108, 124, 139, 140] investigated the full dynamical $\alpha(\omega)$ polarizability and the $\beta(\omega)$, $\gamma(\omega)$ hyperpolarizabilities by QM/MM techniques. In particular, in [136] different CC calculations for the QM part (CC2, CCSD) were tested, using different MM schemes: the dielectric continuum (DC) approach, and the explicit consideration of the water molecules described by a non-polarizable or a polarizable force field. The authors found that CC2 calculations overestimate the second hyperpolarizability *in vacuo*, confirming that γ is strongly affected by electron-correlation effects, while DC models are extremely sensitive to the radius of the cavity into which the water molecule is placed. In their most recent works, the authors have also proposed linear response functions to allow accurate analytical calculations of vibrational contributions to polarizability [138]. Moreover, they extended their CC/MM model to include calculation of statistical averaged quantities [125], finding that the first hyperpolarizability converges slowly and, therefore, requires a more careful sampling with respect to other quantities.

The series of works by Jensen and co-workers [108, 124, 139, 140] also point out the strong influence on the results by the level of description of the MM embedding environment. In particular reference [124], points out the strong differences obtained in the polarizability by using a frozen-density embedding or a discrete reaction field model.

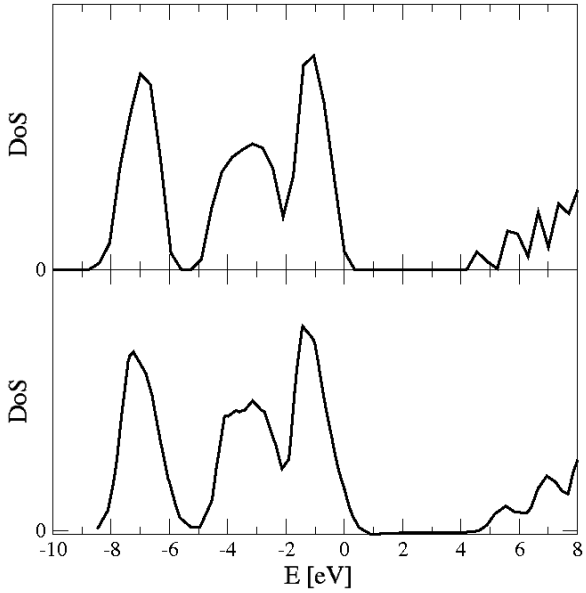

Figure 1. Electronic density of states of liquid water from [144] (upper panel) and from [115] (lower panel).

A recent work by Sonoda *et al* [141] used QM/MM simulations coupling MP2(6-311++G(d, p)) to the SPC/E water model [111] to study the polarizability anisotropy of liquid water. Their calculations managed to reproduce the main features of the experimental frequencies obtained from Kerr effect spectroscopy, but failed to reproduce the experimental band near 60 cm^{-1}.

Despite the promising results described in this section, it seems that the major problem in calculating (hyper)polarizabilities employing QM/MM schemes relies on artifacts generated by the QM/MM interface, especially when using one single water molecule in the QM part. Efforts in characterizing and limiting such undesired effects, e.g. using a larger QM region (for example, one water molecule plus its hydrogen-bonded neighbors) are desired in the near future.

5. Electronic properties

The electronic properties of water, like the density of states and the electronic 'band structure', are extremely interesting and have been the subject of numerous studies. Experimentally, the electronic gap of water has been derived from measurements of the photoionization potential and of the conduction band minimum energy (related to the electron affinity) in photospectroscopy experiments and through the measurements of the magneto-optical interband Faraday rotation [142]. Several theoretical works concerning these properties are also reported in the literature and will be discussed in the following subsection.

5.1. Density of states

The electronic density of states (DoS) of liquid water has been calculated in several theoretical works based on *ab initio* molecular dynamics simulations and DFT [115, 143, 144].

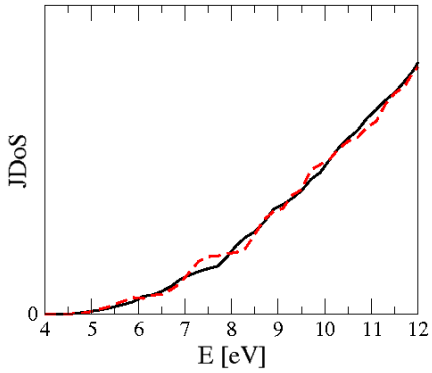

Figure 2. Electronic joint density of states of liquid water for supercells with 17 molecules (red continuous line) and with 32 molecules (black dashed line), from [144].

In [115], DFT-GGA calculations were performed for various water configurations analyzing the convergence of the DoS with respect to the system size and the k-point sampling. For a liquid disordered system increasing the cell size or the number of k-points is not equivalent since there is no periodicity; the more accurate approach would be to use just the Γ point together with a huge unit cell but this strategy is computationally not feasible. In [115], the DoS of a large supercell with 256 water molecules, computed at the Γ point, is found to be in good agreement with the results obtained for a 32 molecule supercell, using eight k-points. Also in [144] the DoSs of liquid water were calculated within DFT-GGA using configurations with 32 molecules obtained from classical molecular dynamics simulations and a Brillouin zone (BZ) sampling of eight k-points. The results of these two calculations (which are in very good agreement with each other) are reported in figure 1.

In both works [115, 144], the electronic joint density of states (JDoS) was also computed for different cell sizes and k-point samplings. The JDoS is a very interesting quantity that gives a first indication of the optical absorption spectrum since it considers all the electronic transitions from unoccupied to occupied states; hence it represents a convolution of the valence and conduction density of states. In figure 2 the JDoS of liquid water is reported for two sizes of the supercell: 17 and 32 water molecules. The two curves are quite similar since, as expected, the JDoS (and hence the optical absorption spectrum) is less sensitive to the system size.

Finally, we mention the work of Boero *et al* [18] where Car–Parrinello molecular dynamics simulations were performed for a hydrated electron in normal and supercritical water and the relative electronic densities of states are reported.

5.2. Electronic energy levels

The experimental electronic gap of liquid water (that is, the difference between the ionization potential and electron affinity) has been estimated to be about 8.7 ± 0.5 eV (see for a detailed review [145, 146] and references therein).

From a theoretical point of view, the electronic 'band structure' of liquid water has been investigated

Table 1. Calculated electronic gaps of various phases of water. The experimental electronic gap of liquid water is 8.7 ± 0.5 eV [145, 146].

	Monomer	Liquid	Ice Ic	Ice Ih
DFT	6.7 eV [22] 6.3 eV [152] 6.16 eV [6]	4.33 eV [115] 5.09 eV [94]	6 eV [148]	5.6 eV [149]
GW	12.5 eV [152]	8.6 eV [94] 8.7 eV [153]		10.1 eV [149]

in detail within DFT-GGA in several works (see for example [22, 94, 115, 144]).

The seminal paper of Laasonen *et al* [22] has shown that, for liquid water, the DFT gap is 4.6 eV, to be compared with the DFT highest occupied molecular orbital–lowest unoccupied molecular orbital (HOMO–LUMO) gap of the monomer (that approximately describes the vapor phase) of 6.7 eV.

The band structure of ice has also been calculated within tight-binding [53, 54, 147], DFT [148, 149], and with the *R*-matrix method [150]. The DFT gap of cubic and hexagonal ice has been evaluated to be 6.0 and 5.6 eV, respectively, i.e. intermediate between liquid and vapor phase.

The difficulty of DFT to quantitatively describe the electronic band structure is well known, as is the fact that DFT electronic gaps, and in general all the DFT single-particle transition energies, heavily underestimate the experimental ones.

The GW approach generally corrects this underestimation (see for example [69, 151]). Recently, GW calculations on liquid water [94, 144], and approximated GW on hexagonal ice [149] and on the monomer [152] have appeared in the literature.

The theoretical values of the electronic gaps of the various phases of water are reported in table 1.

Hydroperoxyl (HO_2) and hydronium (H_3O) radicals have also been considered, for example, in [19] and [154] respectively.

6. Spectroscopic properties

In absorption experiments, light strikes matter and excites an electron from a valence state to a conduction level; therefore there is no change in the total number of electrons: the excited electron remains inside the system and interacts with the corresponding hole. Hence the two particles cannot be treated separately and the joint density of states must be considered. In electron energy loss experiments (EELS) electrons impinge on the sample and lose their energy by exciting electron–hole pairs, plasmons, and other high-order multipair excitations.

The response of a material to radiation is mainly analyzed through its oscillator strength distribution as a function of the probe energy. Different properties of the material, such as reflectance and the optical constants in general, can be obtained from such a distribution. Inelastic x-ray scattering spectroscopy, using hard x-ray radiation, can be used to describe the EEL and, provided that the momentum transfer can be approximated to zero [155], to derive the optical spectra of materials.

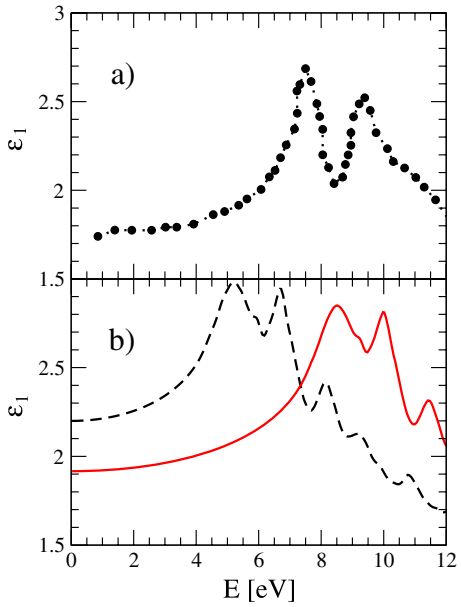

Figure 3. Real part of the electronic dielectric constant ε_1. (a) experimental [158] curve; (b) theoretical [144] curves within DFT (black dashed line) and GW (red continuous line).

Despite decades of efforts, the excited state spectra of liquid water and the influence of solvation on these spectra are still not well understood. In experiments, unlike *in vacuo* UV spectroscopy, the measurement of the absorption spectra of volatile liquids, including water, presents some difficulties. In theoretical calculations, the foremost difficulty is in the choice of an appropriate model for a liquid disordered system that is able to properly include the solvent electronic description and a correct statistical average of the properties of interest.

6.1. Dielectric constant

Optical constants of water (liquid, ice, vapor) have been measured from the far infrared to the high ultraviolet [156–165]. The refraction index $\tilde{n}$ and dielectric function $\tilde{\varepsilon} = \varepsilon_1 + i\varepsilon_2 = \tilde{n}^2$ of liquid water are usually extracted by Kramers–Kronig analyses of reflectance measurements. As an example, we show in figure 3(a) the experimental $\varepsilon_1(\omega)$ for liquid water by Heller *et al* [158].

In the following sections, we will describe in detail the experimental and calculated absorption spectra (related to $\varepsilon_2(\omega)$) of liquid water. Here, we restrict ourselves to the analysis of the electronic dielectric constant ε_∞. Theoretical calculations have been performed within DFT [144], the PPC model [166], the generalized reaction field model of Onsager and discrete local-field theories [167], CASSCF [168], and many-body perturbation theory in the GW approximation [144]. Some of the results present in the literature are reported in table 2.

We see from table 2 that, as expected, DFT overestimates the dielectric constant. This is a direct consequence of the DFT underestimation of the transition energies, as is clear from a comparison of the experimental and DFT spectra (see figure 3). The inclusion of local-field effects slightly reduces the discrepancy with experiment (see table 2). A better

Table 2. Calculated dielectric constant ε_∞. The experimental value, measured at $\omega = 1$ eV, is $\varepsilon_\infty^{\text{exp}} = 1.78$ [158].

Theor. method	Theor. value
PPC [166]	1.25
RF [167]	∼1.69
DFT [144]	2.2
DFT + LF [144]	2.0
DFT + LF [153]	1.72
GW [144]	1.91
CASSCF [168]	1.56 (1.69)

agreement with the experimental value is found within GW, and with more approximate approaches as in [167, 168].

6.2. *Optical absorption*

The first optical absorption experiments on water date back to the 1960s and 1970s [48, 158–160, 169]. In these works the dielectric constants of water, and hence its optical absorption spectrum, were deduced from Kramers–Kronig analyses of reflectance measurements. Other ultraviolet absorption experiments on liquid water were performed in those years, for example in [156, 170–172]. More recently, the optical spectrum of water has been measured by low resolution dipole spectroscopy [173] and by inelastic x-ray scattering spectroscopy [155, 174] at low momentum transfer. Examples of these experimental spectra are shown in figure 4, whereas a closer examination of the low energy region, where excitonic effects are more important, is in figure 5.

The optical absorption spectra of solid water (ice) [163, 169, 175, 176] and of isolated water molecules (vapor) [177–180] or clusters [181] have also been measured.

The spectrum of gas phase water has the first maximum of absorption at 7.4 eV and a second broad band with a maximum at 9.7 eV. At higher energies, many sharper peaks, corresponding to Rydberg transitions, appear. In the condensed phases (liquid water and ice), the sharp Rydberg transitions are not found, while, in the low energy region up to 11 eV, the two broad absorption bands are still present, but blue-shifted with respect to the corresponding bands in the gas phase. In liquid water, the one-photon absorption spectrum shows the first peak at about 8.2 eV, and a second maximum around 9.9 eV. In ice, the first two broad maxima are further shifted to 8.7 and 10.4 eV, respectively. Another characteristic of the liquid water absorption spectrum is the Urbach tail (a long tail present on the red edge of the first band) that is still an object of debate.

The optical absorption spectrum of liquid water has been intensively investigated by theoretical studies. Numerous calculations, performed with different methods and strategies, are present in the literature. The earliest papers on the subject date back to the last century [49, 182–184] and are reviewed in [145, 146]. More recently, several theoretical calculations concerning the vertical excitation energies of liquid water have been reported.

Many of the most recent works consist of QM/MM calculations with one water molecule treated at the quantum level and many others (more than one hundred) treated classically. Within this approach, different combinations of

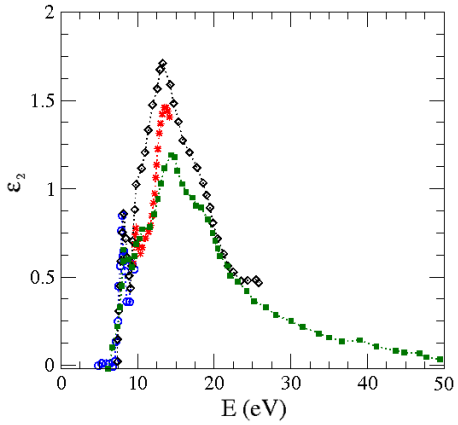

Figure 4. Experimental optical absorption spectra of liquid water from [160] (blue circles), [159] (red stars), [158] (black diamonds), [155] (green squares).

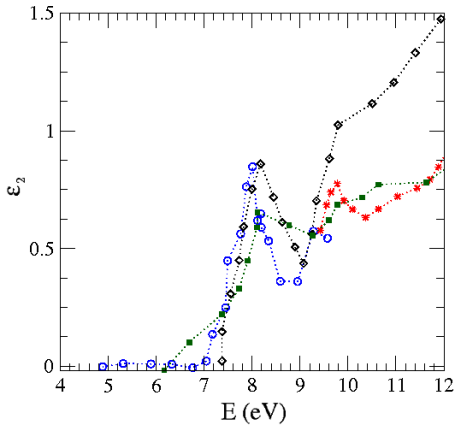

Figure 5. Experimental optical absorption spectra of liquid water from [160] (blue circles), [159] (red stars), [158] (black diamonds), [155] (green squares).

quantum and classical methods can be found; in particular the quantum part has been treated with coupled-cluster theory [109, 125, 133, 135, 185, 186], the multiconfigurational self-consistent-field method [107], DFT [124] and TDDFT [109, 139]. Results obtained with these hybrid QM/MM schemes strongly depend on the details of the calculations: exchange and correlation potentials for both static and time-dependent DFT, basis sets, accuracy in the description of the classical water molecules (continuum models, point charges, polarizable force-fields), or level of approximation in the CC expansion. On average, they present errors in the first few vertical excitation energies within 1 eV with respect to the experimental values.

A different strategy has been followed by Bursulaya and co-workers in [187] where the first photoabsorption band of liquid water is studied by molecular dynamics simulations. In particular they analyze the influence of solvation on the liquid water absorption spectrum with respect to the gas phase. Their results reproduce the main characteristic of the first peak which is found at 8.25 eV, blue-shifted by about 0.5 eV with respect to the lower transition of the vapor and with an extended red tail at lower energies.

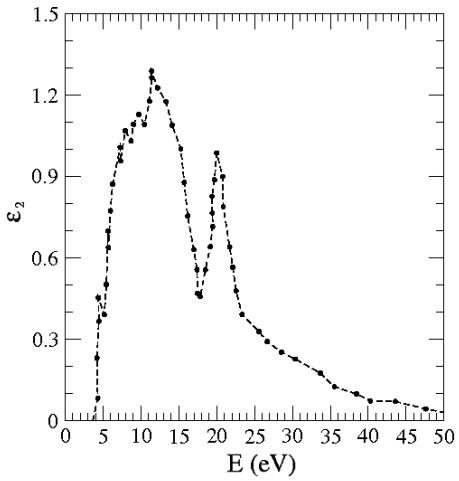

Figure 6. TDDFT imaginary part of the dielectric function, from [188].

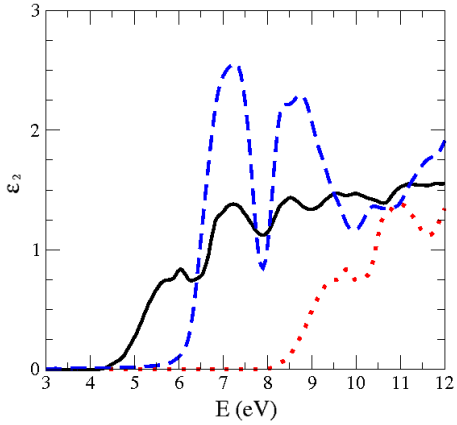

Figure 7. Optical absorption spectrum of liquid water calculated within DFT (solid black line), GW approximation (dotted red line), and by solving the Bethe–Salpeter equation (dashed blue line); from [94].

In [188], the linear response of liquid water is examined through the use of TD-GGA. The liquid system is modeled by one periodically repeated cubic box containing 32 water molecules, with the same density of liquid water at ambient conditions. The electronic properties of water are computed using a real-time propagation scheme for the solution of the TDDFT equations. The imaginary part of the dielectric function, shown in figure 6, is obtained in a wide range of energies. The overall agreement between these results and the experimental absorption spectra is good, especially considering the small number of water molecules considered in the calculation; however, focusing on the low energy part of the spectrum and in particular on the optical gap (onset of the spectrum) the agreement is no longer satisfactory and a significant redshift of the spectrum, with respect to the experiments, is present.

Another theoretical approach for calculating the optical absorption spectrum is given by many-body perturbation theory, through the solution of the Bethe–Salpeter equation. This scheme has been followed in [94]. Also in this work the liquid system has been modeled by a periodically repeated cubic box; however, in this case, several geometrical configurations, each containing 17 water molecules, have been considered and all the results are averaged over these snapshots. In this work the optical spectrum of liquid water has been calculated with different methods: the electronic states have been first obtained within DFT and the relative absorption spectrum is calculated; following this, the energy levels have been corrected within the GW approximation to take fully into account exchange and correlation effects; finally the optical absorption spectrum including excitonic effects has been calculated by solving the Bethe–Salpeter equation. These spectra are shown in figure 7. The DFT optical spectrum shows strong discrepancies with respect to experiment both in the onset and in the lineshape; the overall effect of the GW corrections is to over-shift the DFT spectrum towards higher energies, without improving its shape. The BSE spectrum, on the contrary, shows a significant improvement in the agreement with experiment both in the peak positions and in the onset, as well as in the relative intensities of the first two peaks. The first peak is attributed to a bound exciton with a binding energy of 2.4 eV and large oscillator strength. In [94], the absorption spectrum of liquid water has also been calculated within TDLDA showing no significant improvement with respect to that obtained with DFT-LDA.

Recently, in [6], the optical spectrum of liquid water has been calculated within the symmetry-adapted cluster configuration interaction (SAC-CI), considering a single water molecule in the electric field of surrounding liquid water. Although this model cannot take properly into account the delocalization of the exciton on the surrounding water molecules, the resulting spectrum has a first peak at 8.3 eV in very good agreement with the experimental value of 8.2 eV. The other main structures of the spectrum are also in good agreement with experiments.

A series of theoretical works [6, 181, 186, 189–193] investigated the vertical excitation energies for water clusters of increasing size. This is the case of [189], where the $(H_2O)_n$ clusters, with $n = 2$–6, are studied within Hartree–Fock and second-and fourth-order perturbation theories, whereas in [190] the same clusters have been analyzed with a semi-empirical model. In [186] the vertical excitation energies are calculated with the CC/MM method for the trimer and the pentamer clusters; these clusters and the dimer have also been studied in [191] with CI and CC methods. The optical absorption spectra of larger clusters have been calculated in [192] where a molecular dynamics study of $(H_2O)_n$ clusters, with $n = 8,11, 20, 40, 50$, within the Franck–Condon approximation in the excitonic energy range, is presented.

All these works agree that the first excitation in the clusters is blue-shifted with respect the water monomer and that this blue-shift is larger with increasing cluster size.

A similar analysis has also been made in [181] where the $(H_2O)_n$ clusters and $(H_2O)_{n+1}$ branched clusters, with $n = 2$, 3, 4, 6, have been considered. Apart from the general blue-shift of the first excitation energy with increasing number of water molecules, they also found that this excitation energy is always smaller in the branched structures than in the corresponding

cyclic cluster. In [6], structurally relaxed clusters $(H_2O)_n$, with $n = 2, 3, 5$, are studied within SAC-CI but, unlike the previous cases, after increasing the cluster size, a redshift of the onset of absorption together with a splitting of the main peaks with respect to the monomer spectrum are found. Finally, in [193] the water pentamer is considered in two different geometries, the cyclic cluster and the zwitterionic form and this second structure presents the first absorption peak shifted by more than 1 eV toward smaller energies with respect to the cyclic pentamer.

In some of these works [6, 186, 191] the monomer is also examined as a reference case. Many other theoretical studies have focused on the single H_2O molecule, thus simulating the gas phase of water. Among the earlier works where the excited state properties of the H_2O molecule are considered, we just cite [51, 52, 194, 195]. More recently, the vertical excitation energies of the water molecule have been calculated within TDDFT in [196, 197] and within the Green's function formalism (GW-BSE) in [152]. In this last work the first three transition energies are obtained at 7.24, 9.62, and 10.07 eV, in very good agreement with experimental values.

The solid phase of water, ice, has been the subject of a great number of theoretical studies too; among these we cite the recent work of Hahn and co-workers [149] where the optical absorption spectrum of hexagonal ice has been obtained in the framework of many-body perturbation theory, by including the self-energy corrections in an approximated GW approach [198], and by treating the electron–hole interaction by solving the Bethe–Salpeter equation. The absorption spectrum obtained with these calculations is in good agreement with the experimental one and presents a first peak, at about 9 eV (experimental peak at 8.6 eV), due to a bound exciton with a binding energy of 3.2 eV.

Finally we want to mention a few works devoted to the study of some important radicals that are related to liquid water. The vertical excitation energies of the hydroperoxyl radical, HO_2, important for chemical reactions in the earth's atmosphere, are calculated in [19, 199]. The hydronium radical H_3O and the hydronium–water clusters, interesting for understanding of the behavior of the hydrated electron, are studied in [20, 44, 200]. Lastly, the hydroxyl radical HO that is the primary oxidant in the troposphere and hydroxyl–water clusters are also considered in [40, 201].

6.3. Energy loss

Energy loss spectroscopy is mainly directed at the observation of plasmons, i.e. the collective excitations of electrons as a response to external perturbations. The loss function is related to the dielectric constant through the relation

$$\text{loss} \propto \text{Im}\left(-\frac{1}{\epsilon}\right) = \frac{\epsilon_2}{\epsilon_1^2 + \epsilon_2^2}. \tag{31}$$

The loss function of ice has also been measured by electron energy loss experiments, for example in [202, 203].

Regarding liquid water, the loss function has been obtained in [158] by optical reflectance measurements and, more recently, in [174], from x-ray scattering experiments:

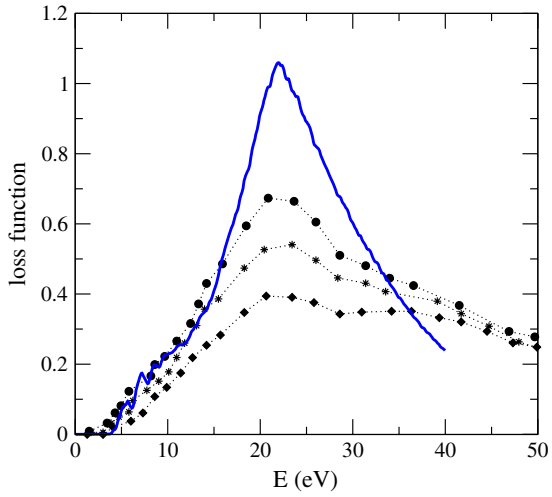

Figure 8. Loss function of liquid water obtained with x-ray scattering measurements for different transferred momenta: $q = 0.19$ (circles), $q = 0.53$ (stars), $q = 0.69$ (diamonds); from [174]. The solid blue line is the loss function of liquid water calculated within DFT for a transferred momentum $q = 0$; from [144].

in both studies the main peak is at an energy (the plasmon frequency) of about 22 eV. The loss spectra presented in [174], for different values of transferred momentum, are shown in figure 8.

The energy loss spectrum of liquid water has been calculated within TD-GGA in [188]. In this work the liquid system was modeled by one periodically repeated cubic box containing 32 water molecules; a value of 21.6 eV is found for the plasmon frequency, in good agreement with experiment.

The energy loss spectrum of liquid water has also been calculated within DFT using a box of 17 water molecules, averaging the results over 20 MD configurations [144]. The averaged spectrum is shown in figure 8, for a transferred momentum $q = 0$. A good agreement with experiment is reached for the peak position and lineshape even if, looking at the onset and in general at the low energy region of the spectrum where excitonic effects are more important, the agreement is less satisfactory.

7. Final remarks

In recent years, the electronic properties of liquid water have been the subject of different computational studies. The constant increase in computational power has allowed scientists both to improve the level of theory for the solution of the quantum problem and to infer statistical averaging to take better into account the properties of the liquid phase. Ground state properties, such as the dipole moment, quadrupole tensor, and dielectric constant have been determined with very good accuracy with respect to the experiment.

Recently, the excited state properties of liquid water have also been computed. These pioneering studies were able to shed light on the main features of the water optical spectrum in the low energy region. In spite of this, however, the large computational costs required for these calculations still call

for drastic approximations that limit the accuracy of the final results. In particular, in reported papers, calculations are typically limited to one single quantum water molecule (in QM/MM studies), or to the first or first–second solvation shell for periodic-cell systems.

All these studies achieve a better description of the electronic and optical properties of liquid water, but still miss a quantitative agreement with experiment. Specifically, electron–hole interactions can be strongly affected by the small system size, leading to over-binding of the excitons and to inaccuracies in the band structures, up to several tenths of an eV.

Development of future techniques, algorithms, and theoretical approaches aimed at decreasing computational costs for excited state calculations are therefore desired for future studies on the subject. Time-dependent LDA and GGA methods represent, at the moment, a quick and valid alternative to many-body perturbation theory in some small molecules and clusters, but fail heavily in describing excitations in extended systems. New TDDFT kernels based on many-body approaches have been successfully used in a variety of systems [88–90, 92, 93] but do not represent, yet, a computationally convenient alternative to a GW plus BSE calculation, since the construction of such non-local and frequency-dependent kernels causes an increase in the computational effort. Promising efficient schemes have been recently proposed [95] which could help in tackling extended systems with a low computational effort (which characterizes TDDFT) while still providing a precise description of many-body effects.

Acknowledgments

We would like to thank Professor Rodolfo Del Sole, Drs Leonardo Guidoni, Conor Hogan, and Margherita Marsili for useful discussions.

References

[1] Wernet P, Nordlund D, Bergmann U, Cavalleri M, Odelius M, Ogasawara H, Näslund L A, Hirsch T K, Ojamäe L, Glatzel P, Pettersson L G M and Nilsson A 2004 *Science* **304** 995
[2] Smith J D, Cappa C D, Wilson K R, Messer B M, Cohen R C and Saykally R J 2004 *Science* **306** 851
[3] Silvestrelli P L and Parrinello M 1999 *J. Chem. Phys.* **111** 3572
[4] Hetenyi B, De Angelis F, Giannozzi P and Car R 2004 *J. Chem. Phys.* **120** 8632
[5] Soper A K, Bruni F and Ricci M A 1997 *J. Chem. Phys.* **106** 247
[6] Hermann A, Schmidt W G and Schwerdtfeger P 2008 *Phys. Rev. Lett.* **100** 207403
[7] Iannuzzi M 2008 *J. Chem. Phys.* **128** 204506
[8] Cavalleri M, Odelius M, Nordlund D, Nilsson A and Pettersson L G M 2005 *Phys. Chem. Chem. Phys.* **7** 2854
[9] Prendergast D and Galli G 2006 *Phys. Rev. Lett.* **96** 215502
[10] Head-Gordon T and Johnson M E 2006 *Proc. Natl Acad. Sci. USA* **103** 7973
[11] Head-Gordon T and Rick S W 2007 *Phys. Chem. Chem. Phys.* **9** 83
[12] Tokushima T, Harada Y, Takahashi O, Senba Y, Ohashi H, Pettersson L G M, Nilsson A and Shin S 2008 *Chem. Phys. Lett.* **460** 387
[13] Leetmaa M, Ljungberg M P, Ogasawara H, Odelius M, Näslund L-A, Nilsson A and Pettersson L G M 2006 *J. Chem. Phys.* **125** 244510
[14] Leetmaa M, Wikfeldt K T, Ljungberg M P, Odelius M, Swenson J, Nilsson A and Pettersson L G M 2008 *J. Chem. Phys.* **129** 084502
[15] Odelius M, Cavalleri M, Nilsson A and Pettersson L G M 2006 *Phys. Rev.* B **73** 024205
[16] Andersson S, Kroes G-J and van Dishoeck E F 2005 *Chem. Phys. Lett.* **408** 415
[17] Andersson S, Al-Halabi A and Kroes G-J 2006 *J. Chem. Phys.* **124** 064715
[18] Boero M, Parrinello M, Terakura K, Ikeshoji T and Liew C C 2003 *Phys. Rev. Lett.* **90** 226403
[19] Iyengar S S 2005 *J. Chem. Phys.* **123** 084310
[20] Sobolewski A L and Domcke W 2002 *J. Phys. Chem.* A **106** 4158
[21] Sprik M, Hutter J and Parrinello M 1996 *J. Chem. Phys.* **105** 1142
[22] Laasonen K, Sprik M, Parrinello M and Car R 1993 *J. Chem. Phys.* **99** 9080
[23] Hofmann D W M, Kuleshova L and D'Aguanno B 2007 *Chem. Phys. Lett.* **448** 138
[24] VandeVondele J, Mohamed F, Krack M, Hutter J, Sprik M and Parrinello M 2005 *J. Chem. Phys.* **122** 014515
[25] Schwegler J C, Grossman E, Gygi F and Galli G 2004 *J. Chem. Phys.* **121** 5400
[26] Grossman J C, Schwegler E, Draeger E W, Gygi F and Galli G 2004 *J. Chem. Phys.* **120** 300
[27] Losada M and Leutwyler S 2002 *J. Chem. Phys.* **117** 2003
[28] Lee H M, Suh S B, Lee J Y, Tarakeshwar P and Kim K S 2000 *J. Chem. Phys.* **112** 9759
[29] Kryachko E S 1999 *Chem. Phys. Lett.* **314** 353
[30] Nielsen I M B, Seidl E T and Janssen C L 1999 *J. Chem. Phys.* **110** 9435
[31] Sadlej J, Buch V, Kazimirski J K and Buck U 1999 *J. Phys. Chem.* A **103** 4933
[32] Severson M W and Buch V 1999 *J. Chem. Phys.* **111** 10866
[33] Jensen J O, Samuels A C, Krishnan P N and Burke L A 1997 *Chem. Phys. Lett.* **276** 145
[34] Estrin D A, Paglieri L, Corongiu G and Clementi E 1996 *J. Phys. Chem.* **100** 8701
[35] Fredericks S Y, Jordan K D and Zwier T S 1996 *J. Phys. Chem.* **100** 7810
[36] Xantheas S S 1995 *J. Chem. Phys.* **102** 4505
[37] Knochenmuss R and Leutwyler S 1992 *J. Chem. Phys.* **96** 5233
[38] Xantheas S S and Dunning T H Jr 1993 *J. Chem. Phys.* **99** 8774
[39] Cooper P D, Kjaergaard H G, Langford V S, McKinley A J, Quickenden T I and Schofield D P 2003 *J. Am. Chem. Soc.* **125** 6048
[40] Crawford T D, Abrams M L, King R A, Lane J R, Schofield D P and Kjaergaard H G 2006 *J. Chem. Phys.* **125** 204302
[41] Engdahl A, Karlström G and Nelander B 2003 *J. Chem. Phys.* **118** 7797
[42] Marshall M D and Lester M I 2005 *J. Phys. Chem.* B **109** 8400
[43] Xie Y and Schaefer H F III 1993 *J. Chem. Phys.* **98** 8829
[44] Sobolewski A L and Domcke W 2002 *Phys. Chem. Chem. Phys.* **4** 4
[45] Cramer C J and Truhlar D G 1999 *Chem. Rev.* **99** 2161
[46] Tomasi J, Mennucci B and Cammi R 2005 *Chem. Rev.* **105** 2999
[47] Lin J, Balabin I A and Beratan D N 2005 *Science* **310** 1311
[48] Williams F, Varma S P and Hillenius S 1976 *J. Chem. Phys.* **64** 1549

[49] Buenker R J and Peyerimhoff S D 1974 *Chem. Phys. Lett.* **29** 253
[50] Borgis D and Staib A 1995 *Chem. Phys. Lett.* **238** 187
[51] Henriksen N E, Zhang J and Imre D G 1988 *J. Chem. Phys.* **89** 5607
[52] Balkova A and Bartlett R J 1993 *J. Chem. Phys.* **99** 7907
[53] Pastori Parravicini G and Resca L 1973 *Phys. Rev.* B **8** 3009
[54] Resca L and Resta R 1977 *Phys. Status Solidi* b **81** 129
[55] Born M and Oppenheimer J R 1927 *Ann. Phys.* **84** 457
[56] Hartree D R 1928 *Proc. Camb. Phil. Soc.* **24** 89
[57] Fock V 1930 *Z. Phys.* **61** 126
[58] Jensen F 1999 *Introduction to Computational Chemistry* (New York: Wiley)
[59] Sherrill C D and Schaefer H F 1999 *Adv. Quantum Chem.* **34** 143
[60] Roos B O 1992 *Lecture Notes in Quantum Chemistry* (New York: Springer)
[61] Olsen J, Roos B O, Jørgensen P and Jensen H J A 1988 *J. Chem. Phys.* **89** 2185
[62] Scuseria G E and Lee T J 1990 *J. Chem. Phys.* **93** 5851
[63] Hohenberg P and Kohn W 1964 *Phys. Rev.* **136** B864
[64] Kohn W and Sham L J 1965 *Phys. Rev.* **140** A1133
[65] Dreizler R M and Gross E K U 1990 *Density Functional Theory* (Berlin: Springer)
[66] Runge E and Gross E K U 1984 *Phys. Rev. Lett.* **52** 997
[67] Gross E K U, Dobson J F and Petersilka M 1996 *Density Functional Theory* (New York: Springer)
[68] van Leeuwen R 2001 *Int. J. Mod. Phys.* B **15** 1969
[69] Onida G, Reining L and Rubio A 2002 *Rev. Mod. Phys.* **74** 601
[70] Becke A D 1988 *Phys. Rev.* A **38** 3098
[71] Lee C, Yang W and Parr R G 1988 *Phys. Rev.* B **37** 785
[72] Perdew J P, Burke K and Ernzerhof M 1996 *Phys. Rev. Lett.* **77** 3865
[73] Langreth D C and Perdew J P 1980 *Phys. Rev.* B **21** 5469
[74] Perdew J P and Wang Y 1986 *Phys. Rev.* B **33** 8800
[75] Perdew J P, Chevary J A, Vosko S H, Jackson K A, Pederson M R, Singh D J and Fiolhais C 1992 *Phys. Rev.* B **46** 6671
[76] Becke A D 1993 *J. Chem. Phys.* **98** 5648
[77] Lembarki A and Chermette H 1994 *Phys. Rev.* A **50** 5328
[78] Todorova T, Seitsonen A P, Hutter J, Kuo I-F W and Mundy C J 2006 *J. Phys. Chem.* B **110** 3685
[79] Santra B, Michaelides A and Scheffler M 2007 *J. Chem. Phys.* **127** 184104
[80] Silvestrelli P L 2008 *Phys. Rev. Lett.* **100** 053002
[81] Dion M, Rydberg H, Schröder E, Langreth D C and Lundqvist B I 2004 *Phys. Rev. Lett.* **92** 246401
[82] Zhao Y and Truhlar D G 2006 *J. Chem. Phys.* **125** 194101
[83] Zhao Y and Truhlar D G 2006 *J. Phys. Chem.* A **110** 13126
[84] Lin I-C, Seitsonen A P, Coutinho-Neto M D, Tavernelli I and Rothlisberger U 2008 *J. Phys. Chem.* B at press
[85] Lin I-C, Coutinho-Neto M D, Felsenheimer C, vonLilienfeld O A, Tavernelli I and Rothlisberger U 2007 *Phys. Rev.* B **75** 205131
[86] vonLilienfeld O A, Tavernelli I, Rothlisberger U and Sebastiani D 2004 *Phys. Rev. Lett.* **93** 153004
[87] Walker B, Saitta A M, Gebauer R and Baroni S 2006 *Phys. Rev. Lett.* **96** 113001
[88] Marini A, Del Sole R and Rubio A 2003 *Phys. Rev. Lett.* **91** 256402
[89] Adragna G, Del Sole R and Marini A 2003 *Phys. Rev.* B **68** 165108
[90] Sottile F, Olevano V and Reining L 2003 *Phys. Rev. Lett.* **91** 056402
[91] Del Sole R, Pulci O, Olevano V and Marini A 2005 *Phys. Status Solidi* b **242** 2729
[92] Pulci O, Marini A and Del Sole R 2008 at press
[93] Varsano D, Marini A and Rubio A 2008 *Phys. Rev. Lett.* **101** 133002
[94] Garbuio V, Cascella M, Reining L, Del Sole R and Pulci O 2006 *Phys. Rev. Lett.* **97** 137402
[95] Sottile F, Marsili M, Olevano V and Reining L 2007 *Phys. Rev.* B **76** 161103R
[96] Reining L, Olevano V, Rubio A and Onida G 2002 *Phys. Rev. Lett.* **88** 066404
[97] Marques M A L, Ullrich C A, Nogueira F, Rubio A, Burke K and Gross E K U 2006 *Time-Dependent Density Functional Theory* (Heidelberg: Springer)
[98] Fetter A L and Walecka J D 1971 *Quantum Theory of Many-Particle Systems* (New York: McGraw-Hill)
[99] Hedin L 1965 *Phys. Rev.* **139** A796
[100] Hedin L and Lundqvist S 1969 *Solid State Phys.* **23** 1
[101] Noell J O and Morokuma K 1975 *Chem. Phys. Lett.* **36** 465
[102] Warshel A and Levitt M 1976 *J. Mol. Biol.* **103** 227
[103] Field M J, Bash P A and Karplus M 1990 *J. Comput. Chem.* **11** 700
[104] Adamovic I and Gordon M S 2005 *Mol. Phys.* **103** 379
[105] Laio A, VandeVondele J and Rothlisberger U 2002 *J. Chem. Phys.* **116** 6941
[106] Kongsted J, Osted A, Mikkelsen K V and Christiansen O 2003 *J. Phys. Chem.* A **107** 2578
[107] Poulsen T D, Ogilby P R and Mikkelsen K V 2002 *J. Chem. Phys.* **116** 3730
[108] Jensen L, van Duijnen P T and Snijders J G 2003 *J. Chem. Phys.* **118** 514
[109] Aschi M, D'Abramo M, Di Teodoro C, Di Nola A and Amadei A 2005 *ChemPhysChem* **6** 53
[110] Errington J R and DeBenedetti P G 2001 *Science* **409** 318
[111] Berendsen H J C, Grigera J R and Straatsma T P 1987 *J. Phys. Chem.* **91** 6269
[112] Rick S W, Stuart S and Berne B J 1994 *J. Chem. Phys.* **101** 6141
[113] Chen B, Xing J H and Siepmann J I 2000 *J. Phys. Chem.* B **104** 2415
[114] Horn H W, Swope W C, Pitera J W, Madura J D, Dick T J, Hura G and Head-Gordon T 2004 *J. Chem. Phys.* **120** 9665
[115] Prendergast D, Grossman J C and Galli G 2005 *J. Chem. Phys.* **123** 014501
[116] Clough S A, Beers Y, Klein G P and Rothman L S 1973 *J. Chem. Phys.* **59** 2254
[117] Shostak S L, Ebenstein W L and Muenter J S 1991 *J. Chem. Phys.* **94** 5875
[118] Coulson C A and Eisenburg D 1966 *Proc. R. Soc.* **291** 454
[119] Tuñón I, Martins-Costa M T C, Millot C and Ruiz-López M F 1995 *J. Mol. Model.* **1** 196
[120] Gregory J K, Clary D C, Liu K, Brown M G and Saykally R J 1997 *Science* **275** 814
[121] Batista E R, Xantheas S S and Jonsson H 1999 *J. Chem. Phys.* **111** 6011
[122] Gubskaya A V and Kusalik P G 2001 *Mol. Phys.* **99** 1107
[123] Kongsted J, Osted A, Mikkelsen K V and Christiansen O 2002 *Chem. Phys. Lett.* **364** 379
[124] Jacob C R, Neugebauer J, Jensen L and Visscher L 2006 *Phys. Chem. Chem. Phys.* **8** 2349
[125] Osted A, Kongsted J, Mikkelsen K V, Åstrand P-O and Christiansen O 2006 *J. Chem. Phys.* **124** 124503
[126] Zeiss G D and Meath W 1977 *Mol. Phys.* **33** 1155
[127] Ward J F and Miller C K 1979 *Phys. Rev.* A **19** 826
[128] Kaatz P, Donley E A and Shelton D P 1998 *J. Chem. Phys.* **108** 849
[129] Levine B F and Bethea C G 1976 *J. Chem. Phys.* **65** 2429
[130] Otto P, Gu F L and Ladik J 1999 *J. Chem. Phys.* **110** 2717
[131] Rodriguez J, Laria D, Marceca E J and Estrin D A 1999 *J. Chem. Phys.* **110** 9039
[132] Maroulis G 2000 *J. Chem. Phys.* **113** 1813
[133] Kongsted J, Osted A, Mikkelsen K V and Christiansen O 2003 *J. Chem. Phys.* **118** 1620
[134] Kongsted J, Osted A, Mikkelsen K V and Christiansen O 2003 *J. Chem. Phys.* **119** 10519

[135] Kongsted J, Osted A, Mikkelsen K V and Christiansen O 2003 *THEOCHEM* **632** 207
[136] Kongsted J, Osted A, Mikkelsen K V and Christiansen O 2004 *J. Chem. Phys.* **120** 3787
[137] Kongsted J, Osted A, Mikkelsen K V, Åstrand P-O and Christiansen O 2004 *J. Chem. Phys.* **121** 8435
[138] Christiansen O, Kongsted J, Paterson M J and Luis J M 2006 *J. Chem. Phys.* **125** 214309
[139] Jensen L, van Duijnen P T and Snijders J G 2003 *J. Chem. Phys.* **119** 3800
[140] Jensen L, van Duijnen P T and Snijders J G 2003 *J. Chem. Phys.* **119** 12998
[141] Sonoda M T, Vechi S M and Skaf M S 2005 *Phys. Chem. Chem. Phys.* **7** 1176
[142] Grevendonk W, Dauwen J, Van den Keybus P and Vanhuyse B 1984 *J. Chem. Phys.* **81** 3746
[143] Hunt P, Sprik M and Vuilleumier R 2003 *Chem. Phys. Lett.* **376** 68
[144] Garbuio V 2006 *PhD Thesis* University of Rome, Tor Vergata
[145] Bernas A, Ferradini C and Jay-Gerin J-P 1997 *Chem. Phys.* **222** 151
[146] Bernas A, Ferradini C and Jay-Gerin J-P 1998 *J. Photochem. Photobiol.* A **117** 171
[147] Zaider M, Fry J L and Orr D E 1989 *Nucl. Tracks Radiat. Meas.* **16** 159
[148] Ching W, Huang M-Z and Xu Y-N 1993 *Phys. Rev. Lett.* **71** 2840
[149] Hahn P H, Schmidt W G, Seino K, Preuss M, Bechstedt F and Bernholc J 2005 *Phys. Rev. Lett.* **94** 037404
[150] Caron L, Bouchiha D, Gorfinkiel J D and Sanche L 2007 *Phys. Rev.* A **76** 032716
[151] Gunnarsson O, Jonson M and Lundqvist B I 1979 *Phys. Rev.* B **20** 3136
[152] Hahn P H, Schmidt W G and Bechstedt F 2005 *Phys. Rev.* B **72** 245425
[153] Lu D, Gygi F and Galli G 2008 *Phys. Rev. Lett.* **100** 147601
[154] Luo M and Jungen M 1999 *Chem. Phys.* **241** 297
[155] Hayashi H, Watanabe N, Udagawa Y and Kao C-C 2000 *Proc. Natl Acad. Sci. USA* **97** 6264
[156] Quickenden T I and Irvin J A 1980 *J. Chem. Phys.* **72** 4416
[157] Kou L, Labrie D and Chylek P 1993 *Appl. Opt.* **32** 3531
[158] Heller J M Jr, Hamm R N, Birkhoff R D and Painter L R 1974 *J. Chem. Phys.* **60** 3483
[159] Kerr G D, Hamm R N, Williams M W, Birkhoff R D and Painter L R 1972 *Phys. Rev.* A **5** 2523
[160] Painter L R, Birkhoff R D and Arakawa E T 1969 *J. Chem. Phys.* **51** 243
[161] Heller J M Jr, Birkhoff R D and Painter L R 1977 *J. Chem. Phys.* **67** 1858
[162] Dingfelder M, Hantke D, Inokuti M and Paretzke H G 1998 *Radiat. Phys. Chem.* **53** 1
[163] Seki M, Kobayashi K and Nakahara J 1981 *J. Phys. Soc. Japan* **50** 2643
[164] Warren S G 1984 *Appl. Opt.* **23** 1206
[165] Zhang J and Grischkowsky D 2001 *Opt. Lett.* **29** 1617
[166] Svishchev I M, Kusalik P G, Wand J and Boyd R J 1996 *J. Chem. Phys.* **105** 4742
[167] Reis H and Papadopoulos M G 2001 *J. Chem. Phys.* **114** 876
[168] Bursulaya B D, Jeon J, Zichi D A and Kim H J 1998 *J. Chem. Phys.* **108** 3286
[169] Onaka R and Takahashi T 1968 *J. Phys. Soc. Japan* **24** 548
[170] Shibaguchi T, Onuki H and Onaka R 1977 *J. Phys. Soc. Japan* **42** 152
[171] Verral R E and Senior W A 1969 *J. Chem. Phys.* **50** 2746
[172] Stevenson D P 1965 *J. Phys. Chem.* **69** 2145
[173] Chan W F, Cooper G and Brion C E 1993 *Chem. Phys.* **178** 387
[174] Hayashi H, Watanabe N, Udagawa Y and Kao C-C 1998 *J. Chem. Phys.* **108** 823
[175] Minton A P 1971 *J. Phys. Chem.* **75** 1162
[176] Dressler K and Schnepp O 1960 *J. Chem. Phys.* **33** 270
[177] Chergui M, Schwentner N and Stepanenko V 1994 *Chem. Phys.* **187** 153
[178] Chergui M and Schwentner N 1994 *Chem. Phys. Lett.* **219** 237
[179] Gurtler P, Saile V and Koch E E 1977 *Chem. Phys. Lett.* **51** 386
[180] Chung C-Y, Chew E P, Cheng B-M, Bahou M and Lee Y-P 2001 *Nucl. Instrum. Methods Phys. Res.* A **467** 1572
[181] Yabushita A, Hashikawa Y, Ikeda A, Kawasaki M and Tachikawa H 2004 *J. Chem. Phys.* **120** 5463
[182] Medina-Llanos C, Ågren H, Mikkelsen K V and Jensen H J A 1989 *J. Chem. Phys.* **90** 6422
[183] Mikkelsen K V, Jørgensen P and Jensen H J A 1994 *J. Chem. Phys.* **100** 6597
[184] Mikkelsen K V and Sylvester-Hvid K O 1996 *J. Phys. Chem.* **100** 9116
[185] Osted A, Kongsted J, Mikkelsen K V and Christiansen O 2004 *J. Phys. Chem.* A **108** 8646
[186] Christiansen O, Nymand T M and Mikkelsen K V 2000 *J. Chem. Phys.* **113** 8101
[187] Bursulaya B D, Jeon J, Yang C-N and Kim H J 2000 *J. Phys. Chem.* A **104** 45
[188] Tavernelli I 2006 *Phys. Rev.* B **73** 094204
[189] Zvereva N A and Ippolitov I I 1997 *Proc. SPIE* **3090** 88
[190] Harvey J N, Jung J O and Gerber R B 1998 *J. Chem. Phys.* **109** 8747
[191] Chipman D M 2005 *J. Chem. Phys.* **122** 044111
[192] Miller Y, Fredj E, Harvey J N and Gerber R B 2004 *J. Phys. Chem.* A **108** 4405
[193] Sobolewski A L and Domcke W 2005 *J. Chem. Phys.* **122** 184320
[194] Morgan L A 1998 *J. Phys. B: At. Mol. Opt. Phys.* **31** 5003
[195] Engel V, Schinke R and Staemmler V 1988 *J. Chem. Phys.* **88** 129
[196] Cai Z-L, Tozer D J and Reimers J R 2000 *J. Chem. Phys.* **113** 7084
[197] Del Puerto M L, Tiago M L, Vasiliev I and Chelikowsky J R 2005 *Phys. Rev.* A **72** 052504
[198] Cappellini G, Del Sole R, Reining L and Bechstedt F 1993 *Phys. Rev.* B **47** 9892
[199] Aloisio S, Li Y and Francisco J S 1999 *J. Chem. Phys.* **110** 9017
[200] Muguet F F, Gelabert H and Gauduel Y 1996 *J. Chim. Phys.* **93** 1808
[201] Schofield D P and Kjaergaard H G 2004 *J. Chem. Phys.* **120** 6930
[202] Michaud M, Cloutier P and Sanche L 1991 *Phys. Rev.* A **44** 5624
[203] Wilson C D, Dukes C A and Baragiola R A 2001 *Phys. Rev.* B **63** 121101